Realization of Celestial Reference Frames using the Allan Variance Classification

C. Gattano, P. Charlot

Abstract Recently [5], a new classification of VLBI radio sources was built on the basis of their astrometric stability revealed by the use of the Allan standard deviation. In such a classification, sources are divided into three groups depending on the nature of the noise content in the astrometric time series. The global level of noise then orders sources within each group. In this proceedings, we present several strategies on the basis of this classification to realize celestial reference frames, i.e. for selecting the set of defining sources used to define the fundamental axes of the frame. This set of sources is usually constrained in the data reduction by a no-net rotation constraint. Using two tools developed to determine the stability of realized frames, one that analyzes the stability of the annual realizations of a given frame and another that analyzes the coherence of random sub-frames, we determine the best usage of this classification.

Keywords Astrometry, celestial reference frame, Allan standard deviation

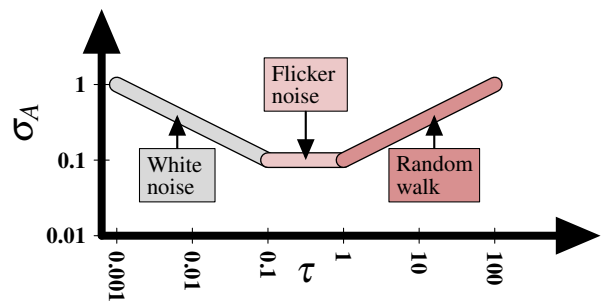

Noise type	Slope in log-log scale	Exponent p in $S_y(f) \propto f^p$	Noise color
Random walk	0.5	-2	Red
Flicker noise	0	-1	Pink
White noise	-0.5	0	White

Table 1 Correspondence between the type of noise, associated with a color given by the exponent of the power law-type spectral density function, and the drift observed in the Allan standard deviation as a function of the timescale represented in a log scale.

1 Introduction

The Allan standard deviation [1] provides a means for measuring the amplitude of the noise as a function of the data averaging timescale from a measurement time series, such as the monitoring of VLBI radio source positions. Initially conceived to characterize the stability of time and frequency standards, the Allan standard deviation has been used in geodesy for about two decades and was raised in several studies aiming at selecting suitable radio sources to define stable celestial frame axes [6, 2, 3, 7] (see also [9] and references therein).

The slope of the Allan standard deviation as a function of the data averaging timescale (in logarithmic scales) discriminates between several types of noise that may coexist in the time series (see the illustration of Table 1). Noise types are separated into two categories:

- Noise types indicating a stable behavior of the series: as the timescale increases, the estimated standard deviation decreases

Laboratoire d'Astrophysique de Bordeaux, Université de Bordeaux, OASU, CNRS

- Noise types indicating an unstable behavior of the series: as the timescale increases, the estimated standard deviation increases as well

The stability of a time series may result from a combination of behaviors associated to different timescale ranges. This principle is at the basis of a recent classification of VLBI radio sources following their assessed astrometric stability from coordinate time series. In the following section, we briefly summarize the principle and the result of this classification. Details are given by Gattano et al. [5].

2 Classification of VLBI Radio Sources

The set of sources is split into three categories following the sequence of the dominating noise at each timescale, i.e. with respect to the behavior of the data at those timescales:

- **AV0** sources with the most stable astrometric behavior. The condition to be classified as AV0 is not to be dominated by unstable noise (slope larger than +0.25, see Table 1) such as red noise at any timescale.
- **AV1** intermediate astrometric stability. AV1 is dominated by unstable noise at some timescales, but stable noise (slope lower than -0.25, see Table 1) such as white noise dominates on the longest timescales appreciable considering the observational history of the source.
- **AV2** sources with the least stable behavior. All sources for which the longest timescales are dominated by an unstable noise.

Right ascension and declination are studied separately. The source category is obtained by keeping only the worst category. Additionally, the global level of noise is evaluated taking into account the straight line that maximizes the Allan standard deviation graph (see the blue line in Figure 1). By doing so, it is possible to order sources within each category by increasing level of noise.

In parallel, a statistical validation test is used to determine the probability that the detected slope results from a white noise process even if it is not -0.5 (due to the irregularity of the sampling). It is based on Monte-Carlo simulations of 1,000 white noise draws distributed on the original sampling of the tested time series. The scatter of their corresponding Allan standard deviations provides an empirical error (see Figure 1 for example). Thanks to this test, each of the un-

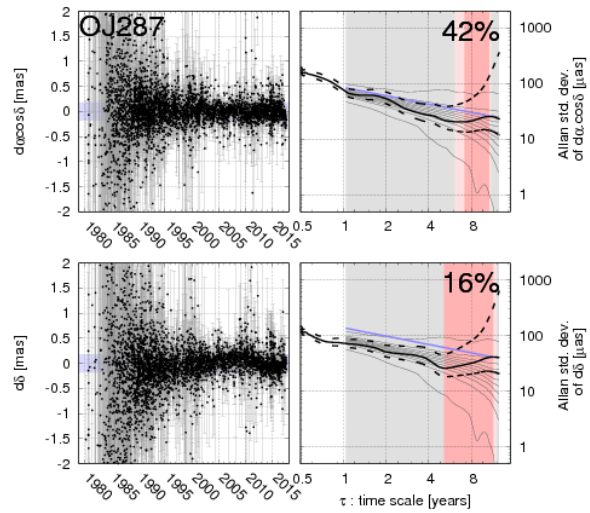

Fig. 1 (Left) Astrometric offset with respect to the mean position computed for each VLBI session. (Right) Allan standard deviation of the regularized time series over time scale τ. The log-log diagram is plotted with a black solid line with its uncertainties at 90% as black dashed lines. The colored background indicates the behavior of the noise at each time scale (more details are in Section 1). The blue straight line is the lowest line that maximizes the diagram down to $\tau = 1$ year. It leads to the global noise level of the source (more details are in Section 2). The grey solid lines are the dispersion of the Monte-Carlo test (more details are in Section 2). How much the black diagram remains within the dispersion lines provides the indicated probabilities on the top right corners. They are compared with the threshold of the rehabilitation process.

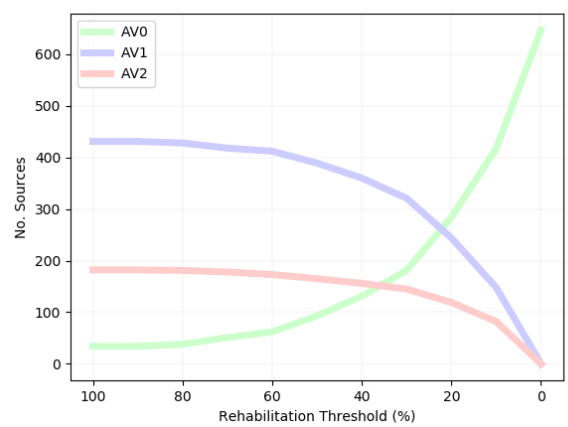

Fig. 2 Evaluation of the source distribution within the classification with respect to the chosen rehabilitation threshold (more details on the text on right).

stable sources (AV1/2) has therefore a certain probability to be in fact a stable source (AV0) offering the possibility to rehabilitate some sources for which their probability is greater (on both coordinates) than a given threshold. Figure 2 shows the evolution of the classification as the threshold varies.

3 Stategies to Select Defining Sources

We establish several strategies to realize celestial reference frames by selecting the set of defining sources. Table 2 below sums up the criteria for each strategy:

- N is the number of defining sources to be selected;
- P_{rehab} is the chosen rehabilitation threshold (see Section 2);
- σ_{AV0}, σ_{AV1}, and σ_{AV2} are upper limits for the noise level in each category (10 mas enables exclusion of all sources);
- $prior = 0$ gives the priority on the source class (data behavior) for the selection and then on the noise level. $prior = 1$ is reversed.

No. sol.	N	P_{rehab} [%]	σ_{AV0} [mas]	σ_{AV1} [mas]	σ_{AV2} [mas]	$prior$
GROUP 1: Only AV0 sources						
1	100	50	10	0	0	0
2	100	25	10	0	0	0
3	200	25	10	0	0	0
4	100	0	10	0	0	0
5	200	0	10	0	0	0
6	300	0	10	0	0	0
7	400	0	10	0	0	0
8	500	0	10	0	0	0
GROUP 2: First AV0, then AV1, no AV2						
9	200	50	10	10	0	0
10	300	50	10	10	0	0
11	300	25	10	10	0	0
GROUP 3: smallest level of noise						
12	100	-	10	10	10	1
13	200	-	10	10	10	1
14	300	-	10	10	10	1
15	400	-	10	10	10	1
16	500	-	10	10	10	1
GROUP 4: smallest level of noise but no AV2						
27	100	50	10	10	0	1
28	200	50	10	10	0	1
29	300	50	10	10	0	1
30	100	25	10	10	0	1
31	200	25	10	10	0	1
32	300	25	10	10	0	1
33	100	0	10	10	0	1
34	200	0	10	10	0	1
35	300	0	10	10	0	1
36	400	0	10	10	0	1
37	500	0	10	10	0	1

Table 2 List of realization strategies of celestial reference frames based on the classification of Gattano et al. [5]. See the text for the meaning of each column. The representative of each group is highlighted in light blue.

For each solution, the criteria are used within the following way.

First, we rehabilitated AV1/2 sources into the AV0 category regarding the chosen P_{rehab} threshold. Then, we excluded sources in each category which have a level of noise greater than the chosen σ_{AVi}. Then, if $prior = 0$, we selected the first N remaining AV0 sources. When there are no more AV0 sources, we continue with the remaining AV1 sources and then the remaining AV2 sources. If $prior = 1$, we first gathered all remaining sources and ordered them according to their noise level. Then, we selected the first N ones.

4 Method to Analyze the Stability of Celestial Reference Frames

We developed two statistical tools to assess the stability of celestial reference frames. Each of these is associated with a different concept of the stability of a frame.

4.1 Stability over Time

The Allan standard deviation analysis revealed that only a limited number of sources have stable behavior (see Figure 2). Every other one shows a perceptible variability affecting its astrometric position. Consequently, "how far can we state the non-rotation or non-deformation of the frame over time?" is a fundamental question when investigating the stability of the celestial reference frame. One difficulty is that we do not have the capability to measure the true stability of the frame because we cannot observe frequently the whole subset of defining sources.

Through the source observational history, we can nevertheless get some insights into the frame stabilities over time. We quantified this insight on an an-

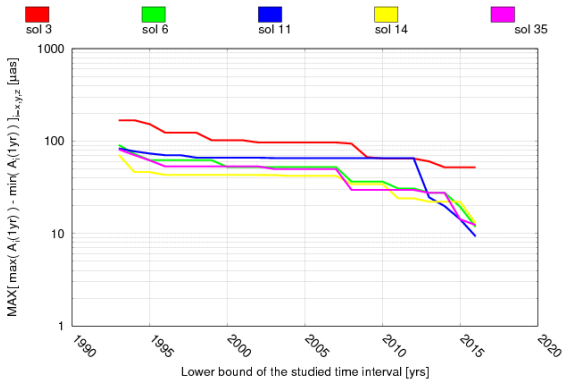

Fig. 3 Comparison of the quantifiable part of the annual stability between representatives of each solution group (see Section 3). From annual rotation time series $A_i(t)$ ($i = x$ for rotation around (Ox) axis, $i = y$ around (Oy), and $i = z$ around (Oz)), we chose the comparison criterion as the maximum between the largest differences within each of the three time series. The comparison criterion is computed on a time interval delimited by a chosen epoch up to the most recent date in the data. The value of this lower limit is given in abscissa and the related comparison criterion in ordinate in μas.

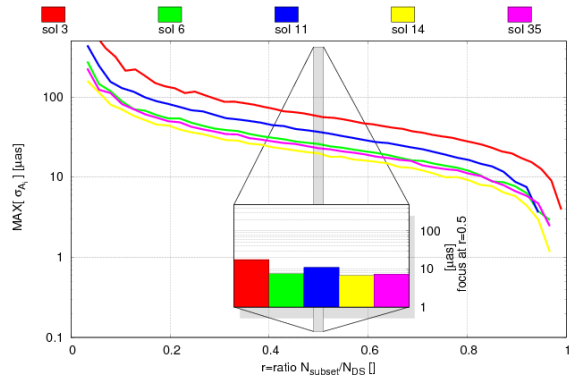

Fig. 4 Comparison of the sub-frame orientation dispersion between representatives of each solution group (see Section 3). The comparison criterion is set on the maximum between the three standard deviations σ_{A_i} ($i = x$ for rotation around (Ox) axis, $i = y$ around (Oy), and $i = z$ around (Oz)) of the thousand random sub-frames of size $N_{subset} \in [0 : N_{DS}]$, N_{DS} being the total number of defining sources of the complete frame.

nual basis by computing annual versions of celestial frame solutions by means of the annually-averaged positions of the observed sources. Then, we assessed the differences between these annual frames by comparing the rotation parameters $A_x(t)$, $A_y(t)$, and $A_z(t)$ between these frames. Finally, the stability is derived from the maximum of the differences on a time-interval with a given lower limit. In Figure 3, we show one of the three rotation parameters with the largest difference depending on the chosen lower time limit. For legibility, we only plot representatives of each group of solutions.

4.2 Sub-frames Orientation Coherence

On the other hand, only a subset of N sources among the set of N_{DS} defining sources is observed during a VLBI session, and the frame orientation within the session is determined to a certain extent by this sub-frame. "Whether the sub-frame has statistically the same orientation as the complete frame" is also an important question when dealing with frame stability.

Therefore, we randomly drew a thousand times N_{subset} sources from the total set of N_{DS} defining sources of a celestial frame solution (see Section 3). In other words, we got a thousand random sub-frames of identical size. We computed their statistical relative differences in orientation and retrieved the standard deviation on each rotation parameter A_x, A_y, and A_z. We repeated the process with different values of ratio N_{subset}/N_{DS} and drew the function of this standard deviation with respect to the ratio N_{subset}/N_{DS} (see Figure 4). For legibility, we only plot representatives of each group of solutions in Figure 4.

As a result, it is the height of this function with respect to the standard deviation axis which differs, more than the shape of curve. The height may be different between axes of different celestial frames but also between the three axes of the same frame. The most stable celestial frame shows the lowest height when considering all the three axes together, which means the lowest dispersion between the set of random sub-frames.

5 Results and Discussion

Based on the two statistical tools used (see Section 4), we note that the "sol 3", representative of the group *"Only AV0 sources"* is curiously the least stable celestial frame. AV0 sources, although having a stable behavior, present in general a higher level of noise. As the whole set of defining sources in "sol 3" are AV0, this explains its last position in the comparison.

On the opposite end, "sol 14", as the representative of the group where only the level of noise of the sources is taken into account to select defining sources, is the most stable celestial frame in the comparison. This leads to the conclusion that, for the realization of a celestial frame at a determined epoch, the dominant information to take into account is the noise level of the sources. The data behavior only comes in second rank for the selection of defining sources.

The ranking between representative solutions goes in the same sense:

- "sol 11" better than "sol 3" shows the advantage of taking AV1 sources into account, and
- "sol 14" better than "sol 35" shows the disadvantage of excluding AV2 sources;

as well as the differences between solutions within each group:

- "sol 5" (non-plotted) better than "sol 3", "sol 11" better than "sol 10" (non-plotted), and "sol 35" best of its group show the advantage to lowering the rehabilitation threshold P_{rehab} to its minimum value, 0%, which is equivalent to making the division AV0/AV1/AV2 meaningless.

Another conclusion is the confirmation that a total of about 300 sources is enough to obtain optimal stability performance in the realization of a celestial reference.

By the time we wrote those lines, the IAU working group in charge of the realization of the third version of the international celestial reference frame finalized its work, and the resulting ICRF3 was adopted by the IAU during the XXX General Assembly as the next celestial reference frame (which will come into effect on the 1st of January, 2019).

In the meantime, what was not addressed in this study, as well as during the realization of the two previous versions of ICRF [8, 4], is the assessment, at the time of realization, of the defining source behavior impact on the future evolution of the celestial frame. In other words, is it possible to assess, when selecting the defining sources, their effect on the frame stability due to individual instabilities that may come in the future? Data behavior revealed by the use of the Allan standard deviation might be of great help in this task, but further investigations are needed to confirm this possibility. The almost 40 years of VLBI observations should be of great value for such studies.

Acknowledgements

This work has been supported by a CNES post-doctoral grant. César Gattano is grateful to the IAG, the CNFGG and the OASU for supporting the trip and thus allowing the presentation of this work at the IVS General Meeting.

References

1. Allan, D. W., Statistics of atomic frequency standards, IEEE Proceedings, 1966, 54, 221-230.
2. Feissel-Vernier, M., Selecting stable extragalactic compact radio sources from the permanent astrogeodetic VLBI program, A&A, 2003, 403, 105-110.
3. Feissel-Vernier, M.; de Viron, O. & Le Bail, K., Stability of VLBI, SLR, DORIS, and GPS positioning, Earth, Planets, and Space, 2007, 59, 475-497.
4. Fey, A. L.; Gordon, D.; Jacobs, C. S.; Ma, C.; Gaume, R. A.; Arias, E. F.; Bianco, G.; Boboltz, D. A.; Böckmann, S.; Bolotin, S.; Charlot, P.; Collioud, A.; Engelhardt, G.; Gipson, J.; Gontier, A.-M.; Heinkelmann, R.; Kurdubov, S.; Lambert, S.; Lytvyn, S.; MacMillan, D. S.; Malkin, Z.; Nothnagel, A.; Ojha, R.; Skurikhina, E.; Sokolova, J.; Souchay, J.; Sovers, O. J.; Tesmer, V.; Titov, O.; Wang, G. & Zharov, V., The Second Realization of the International Celestial Reference Frame by Very Long Baseline Interferometry, Astron. J., 2015, 150, 58.
5. Gattano, C.; Lambert, S. B. & Le Bail, K., Extragalactic radio source stability and VLBI celestial reference frame: insights from the Allan standard deviation, A&A, 2018, accepted.
6. Gontier, A.-M.; Le Bail, K.; Feissel, M. & Eubanks, T. M., Stability of the extragalactic VLBI reference frame, A&A, 2001, 375, 661-669.
7. Le Bail, K.; Gordon, D. & Ma, C., Selecting Sources that Define a Stable Celestial Reference Frame with the Allan Variance, International VLBI Service for Geodesy and Astrometry 2016 General Meeting Proceedings: "New Horizons with VGOS", Eds. Dirk Behrend, Karen D. Baver, Kyla L. Armstrong, NASA/CP-2016-219016, p. 288-291, 2016.
8. Ma, C.; Arias, E. F.; Eubanks, T. M.; Fey, A. L.; Gontier, A.-M.; Jacobs, C. S.; Sovers, O. J.; Archinal, B. A. & Charlot, P., The International Celestial Reference Frame as Realized by Very Long Baseline Interferometry, Astron. J., 1998, 116, 516-546.
9. Malkin, Z., Application of the Allan Variance to Time Series Analysis in Astrometry and Geodesy: A Review, IEEE Transactions on Ultrasonics Ferroelectrics and Frequency Control, 2016, 63, 582-589.